

Enhanced corrosion resistance of phytic acid coated magnesium by stearic acid treatment

R. K. GUPTA, K. MENSAH-DARKWA, J. SANKAR, D. KUMAR

Engineering Research Center for Revolutionizing Metallic Biomaterials (ERC-RMB),
North Carolina A&T State University, 1601 East Market Street, Greensboro, NC-27411, USA

Received 2 July 2012; accepted 5 November 2012

Abstract: A green chemical conversion coating for magnesium was obtained with a phytic acid solution. The microstructure and corrosion properties of phytic acid conversion coated magnesium were further improved by soaking in stearic acid solution. The phytic acid conversion coated magnesium after soaking in the stearic acid showed no micro-cracks and the surface became very smooth. The corrosion behavior of the uncoated and coated magnesium samples was studied by electrochemical methods. The corrosion resistance of the stearic acid treated sample was much higher than that of phytic acid conversion coated magnesium or uncoated magnesium. The electrochemical results indicated that the stearic acid treated coating provided effective corrosion protection to the magnesium sample.

Key words: magnesium; phytic acid; stearic acid; corrosion; impedance spectroscopy

1 Introduction

Magnesium and its alloys have attracted considerable research attention because of their light weight, high specific strength, castability, biocompatibility, and natural abundance [1–4]. Due to these unique properties, they are considered to be very promising candidate for biomedical, automobile, and aeronautical applications [5–7]. However, high corrosion rate of magnesium and its alloys limits their extensive utilization. Surface modification is one of the effective methods to improve the corrosion resistance of magnesium and its alloys. The main focus of the surface modification of magnesium is to reduce its corrosion rate [8,9], understand the coating mechanism [10,11], and enhance its application in biological implants [12–14].

Among the various surface modification techniques, chromate conversion coating is a very popular and effective method [15,16]. However, due to the environmental impact of hexavalent chromium ion and the imminence of associated restrictions, there is a high demand for the development of less harmful and environment friendly surface treatment method [17]. Recently, phytic acid (PA) has emerged as an alternative green surface modification technique to prevent the

corrosion of magnesium [18]. Phytic acid ($C_6H_{18}O_{24}P_6$), a non-toxic naturally occurring organic acid, is biocompatible and environment friendly [19,20]. It is found in most legumes such as corn, nuts, and soy beans [19,21]. The active groups of phytic acid can react with metal ions such as magnesium, and form stable chelate compounds on the surface of magnesium which can slow down the corrosion rate of magnesium [22,23].

LIU et al [22] have studied the effect of immersion time, temperature, pH value, and concentration of phytic acid on the corrosion resistive behavior of phytic acid coated magnesium alloy. It was observed that the corrosion resistance of phytic acid conversion coating was comparable with the chromate conversion coating. CUI et al [24] have observed micro-cracks in the phytic acid conversion coated magnesium alloys which impair the corrosion resistance of the coating. It was also reported that the thickness of the phytic acid coating increased with the increase in the immersion time, but the thicker film had more micro-cracks.

In this work, we have tried to reduce the micro-cracks in the phytic acid conversion coated magnesium by post treatment with stearic acid [$CH_3(CH_2)_{16}COOH$]. Stearic acid (SA) is a long-chain saturated fatty acid which is the main component of fat. It is nontoxic and biocompatible [25,26]. The effect of stearic acid post

treatment on the corrosion behavior of magnesium was studied. Potentiodynamic polarization and electrochemical tests were performed to study the corrosion behavior of the uncoated magnesium and phytic acid conversion coated magnesium with and without the stearic acid treatment. It was found that the stearic acid treatment reduces the micro-cracks in the phytic acid conversion coating, and in turn reduces the percolation and permeation of reactive ions in the solution to magnesium substrate and thus improves the corrosion resistive property of the coating.

2 Experimental

The magnesium sample for the coating was prepared by cutting high purity magnesium (99.9%) rod (GoodFellow, Germany) into 2.54 cm circular disc with a thickness of ~1.1 mm. Prior to the phytic acid conversion coating, the magnesium sample was progressively polished with SiC paper up to grade #1200, followed by degreasing in acetone. The phytic acid conversion coating was formed by dipping the magnesium sample in the phytic acid solution (50% H₂O) at room temperature for 3 h. The immersion time (3 h) has been found to be optimum to yield coatings with the lowest corrosion current density during the potentiodynamic polarization study. The longer immersion of magnesium in the phytic acid resulted in more cracking in the coating and thus higher corrosion current density. After that, the samples were taken out from the phytic acid solution and were washed with deionized water. The samples were dried at 60 °C for 3 h. The post treatment of the coated magnesium was done by immersing in stearic acid (Sigma-Aldrich, USA) solution (1 mg/mL in ethanol) for 2 h at 80 °C. Hereafter, uncoated Mg, PA coated Mg, and PA-SA coated Mg represent uncoated magnesium, phytic acid conversion coated magnesium, and stearic acid treated phytic acid conversion coated magnesium, respectively. The schematic diagram of the coating process is shown in Fig. 1. Being a very simple immersion coating process, this coating technique can be adopted for different shaped magnesium samples. The thickness of the phytic acid conversion coated magnesium was measured with a cross-section scanning electron microscope and was observed to be ~ 2.3 μm (Fig. 2). The microstructures of the bare and coated magnesium samples were recorded before and after corrosion process with the scanning electron microscope (SEM, SU8000, Hitachi). The energy dispersive X-ray spectroscopy (EDS, Quantax 200, Bruker) was used to examine the elemental compositions of the coating. The adhesion of the coatings to the magnesium substrate was measured using the ASTM (American Society for Testing and Materials, Pennsylvania, USA) standard

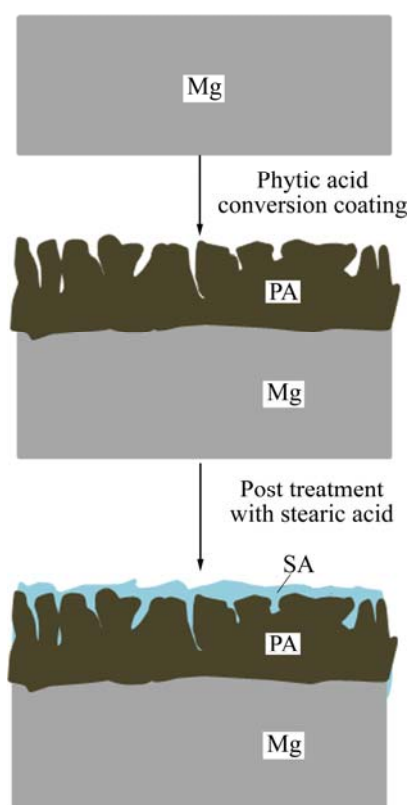


Fig. 1 Schematic diagram of coating process

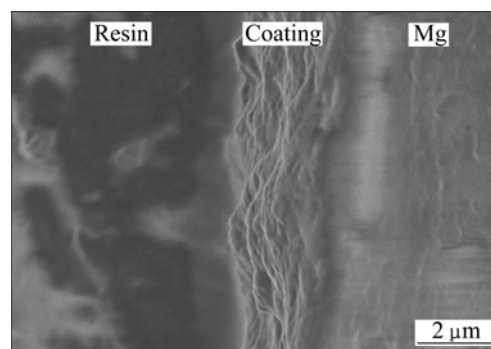


Fig. 2 Cross-section SEM image of PA conversion coated magnesium

D3359-02 tape test with a pressure-sensitive tape (Elcometer 99, ASTM D3359 Tape). DC potentiodynamic polarization measurements were performed in 1×phosphate buffered saline (PBS) solution (137 mmol/L NaCl, 2.7 mmol/L KCl, 8 mmol/L NaHPO₄ and 2 mmol/L KH₂PO₄) using Gamry Potentiostat (R600, Gamry Instruments) with a standard three-electrode configuration. Ag/AgCl (saturated KCl) and platinum wire were used as the reference and counter electrodes, respectively. Uncoated and coated magnesium samples were used as the working electrode. All the measurements were carried out at room temperature. Corrosion potential (ϕ_{corr}) and corrosion current density

(J_{corr}) were determined using the Echem Analyst software (Gamry Instruments). The electrochemical impedance spectroscopy (EIS) study was performed in the frequency range of 0.1– 10^6 Hz under 10 mV amplitude of the perturbation signal.

3 Results and discussion

The chemical composition of the PA coated magnesium sample was analyzed using EDS. The EDS spectrum of the sample is shown in Fig. 3. As seen in the spectrum, the phytic acid coating was mainly composed of Mg, O, P, and C elements, and the presence of P in the coating showed that phytic acid was successfully conversion coated on the magnesium surface [18]. The microstructures of the uncoated magnesium, PA coated magnesium, and PA-SA coated magnesium samples are shown in Fig. 4. These microstructures were taken before or after the corrosion study. As evident from these microstructures, PA coated magnesium showed the presence of micro-cracks. Such kind of micro-cracks

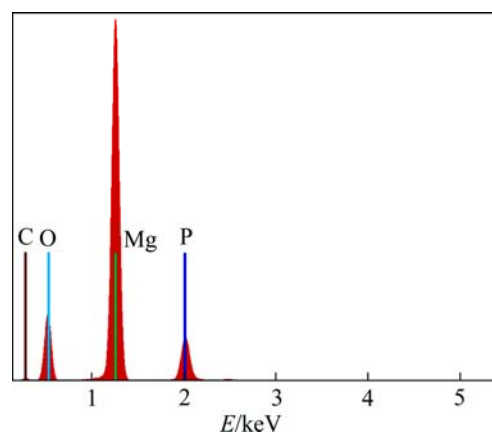


Fig. 3 EDS spectrum of PA conversion coated magnesium

were reported by others also [24]. As seen in Fig. 4, soaking in stearic acid solution improves the surface properties of phytic acid conversion coated magnesium. The micro-cracks presented in phytic acid conversion coated magnesium disappeared after soaking in the

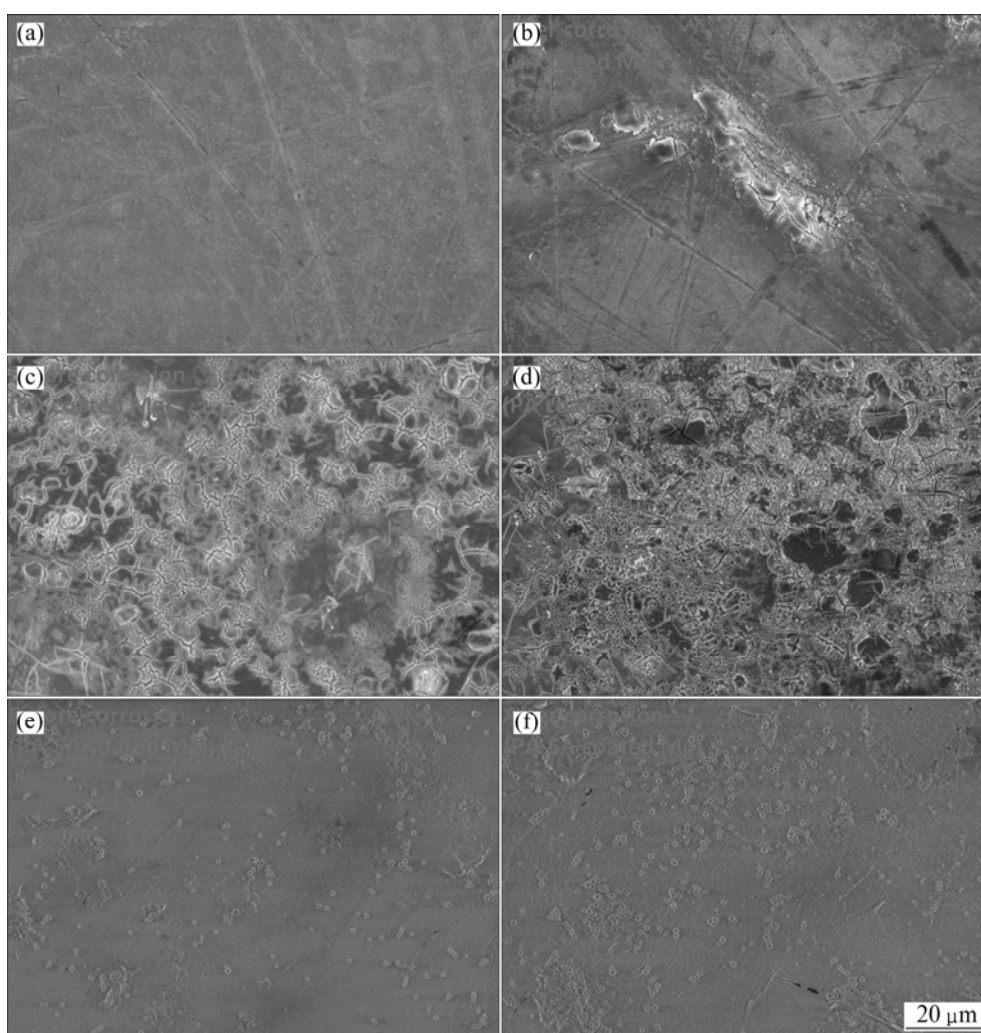


Fig. 4 SEM images of uncoated magnesium (a, b), PA conversion coated magnesium (c, d), and PA-SA coated magnesium (e, f) samples before (a, c, e) and after (b, d, f) corrosion

stearic acid. The smoothness of the surface resulted from the filling of micro-cracks with the stearic acid solution. The absence of micro-cracks in the stearic acid treated sample reduces the penetration of reactive ions from solution to magnesium substrate, which reduces the corrosion of magnesium.

The adhesion properties of the coating to the magnesium substrate were studied by an adhesion test. Subjecting the coating to the adhesion test is very important to determine the quality of the coating for its useful applications. Low quality coating can peel off from the substrate and thus cannot provide sufficient protection to the substrate. The ASTM tape test was performed to study the adhesion strength of the coatings on the magnesium substrate [27]. Figure 5 shows the optical images of the cross cut patterns on PA coated magnesium and PA-SA coated magnesium samples before the application of the tape and after the application and then removal of the tape from the samples. As was evident from these figures, almost the whole coating was undetached after the removal of the tape from the samples. This indicates that these coatings have strong adhesion to the magnesium substrate. In the next sections, we will present the effect of stearic acid post treatment on the corrosion properties of phytic acid conversion coated magnesium substrate.

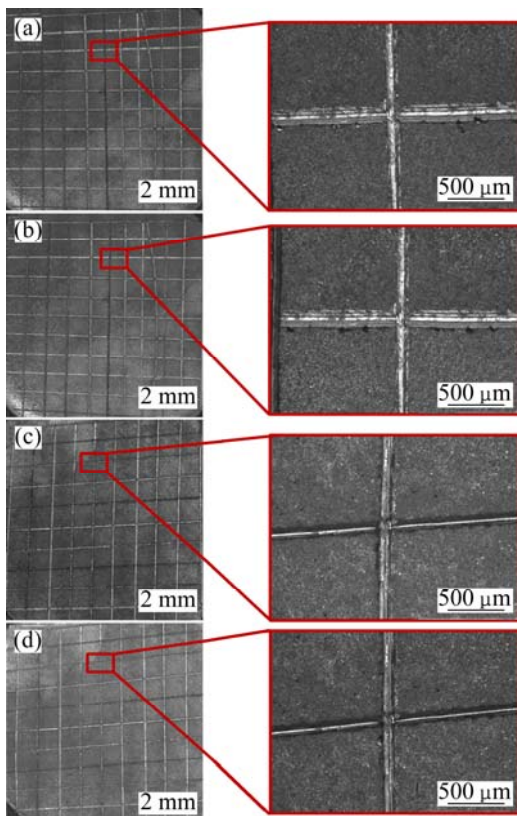


Fig. 5 Optical images before (a,c) and after (b, d) adhesion test for PA conversion coated magnesium (a, b) and PA-SA coated magnesium (c, d) substrates, respectively

Potentiodynamic polarization measurements were used to study the corrosion behavior of uncoated magnesium, PA conversion coated magnesium, and PA-SA coated magnesium samples. Before recording the measurements, the samples were immersed in the PBS solution for 15 min to attain steady state reaction condition. The steady state corrosion reaction condition was verified by monitoring open-circuit potential. PBS solution was used for these studies as the ionic concentrations of the PBS solution are very close to those of body fluid except it does not contain proteins [28]. As the corrosion of metallic implant occurs due to the presence of these ions, in-vitro reactivity characterizations will help to understand the degradation processes (failure risks) and the development of new implant materials [29]. Screening the samples first in-vitro in simulated environment will also help us to reduce the cost involved in testing the implants in-vivo for degradation study. The polarization studies were carried out in the applied potential range of ± 300 mV (vs SCE), at 5 mV/s scan rate. The potentiodynamic polarization curves for uncoated and coated magnesium are shown in Fig. 6. As seen from the polarization curves, the corrosion potential of the coated magnesium shifted positively. It was also observed that the corrosion current density for the coated magnesium decreased. The values of the corrosion potential and corrosion current density were estimated by the Stern-Geary equation [30]:

$$J_{\text{corr}} = \frac{1}{2.303R_p} \left(\frac{\beta_a \times \beta_c}{\beta_a + \beta_c} \right) \quad (1)$$

where β_a is the anodic Tafel slope; β_c is the cathodic Tafel slope and R_p is the polarization resistance. The calculation of Tafel slopes is based on the mixed potential theory [31]. When a corroding specimen is polarized by an applied current, the anodic and cathodic polarization curves meet at ϕ_{corr} . At current densities high

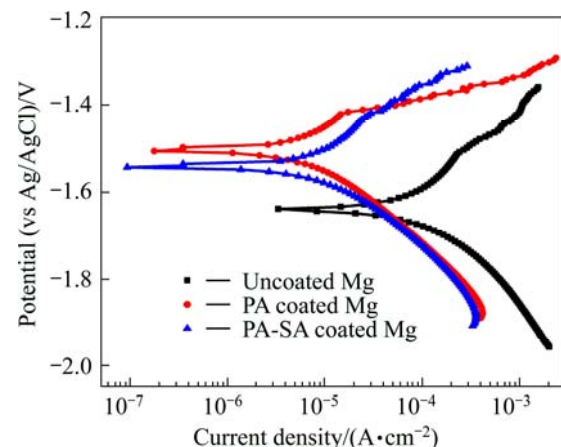


Fig. 6 Potentiodynamic polarization curves for uncoated and coated magnesium samples

enough, the curves become linear on a semi-logarithmic plot. The linear portions of the curves were extended over lengths greater than one order of magnitude to endure accuracy in the extrapolation and determination of the Tafel constants (β_a and β_c) [32]. The polarization resistance (R_p) of the samples was calculated using Eq. (2):

$$R_p = \left(\frac{\partial \Delta E}{\partial I} \right)_{J=0, dE/dt \rightarrow 0} \quad (2)$$

where J is the current density. The corrosion rate (η) of the samples is calculated using J_{corr} (from Eq. (1) and (3)):

$$\eta = \frac{3.28m_e}{\rho} J_{\text{corr}} \quad (3)$$

where m_e is the equivalent mass of magnesium, ρ is density, and J_{corr} is corrosion current density (mA/cm^2). As seen in Eq. (3), corrosion rate is directly proportional to J_{corr} , namely, a lower corrosion current density means a lower corrosion rate of the sample. The corrosion current densities for uncoated magnesium, PA conversion coated magnesium, and PA-SA coated magnesium were calculated to be 3.14×10^{-5} , 1.16×10^{-6} , 1.03×10^{-6} A/cm^2 , respectively. Based on the corrosion current densities, the corrosion rates of uncoated magnesium, PA conversion coated magnesium, and PA-SA coated magnesium were calculated to be 0.717, 0.027, and 0.024 mm/a, respectively. This indicates that post treatment of PA coating with stearic acid decreases the corrosion rate of magnesium sample. On the other hand, the corrosion potentials for uncoated magnesium, PA conversion coated magnesium, and PA-SA coated magnesium samples were observed to be -1.64 , -1.50 , and -1.54 V, respectively. The positive shift in the corrosion potential indicates moving toward nobleness. These results indicate that the PA and PA-SA coated magnesium samples are more cathodic and corrosion protective in nature compared to the uncoated magnesium.

The corrosion protective nature of the coatings was analyzed further using electrochemical impedance spectroscopy (EIS). The EIS measurements were recorded at the open circuit potential after stabilizing in the PBS solution for 15 min. The effects of coatings on the electrochemical impedance data for various samples are shown in Fig. 7. As seen in the Nyquist plots (Fig. 7(a)) of these samples, a larger radius of curvature was observed for the coated magnesium samples than the uncoated magnesium. It was also observed that the radius of curvature for PA-SA coated magnesium was the largest that was followed by PA conversion coated magnesium and uncoated magnesium samples. The largest radius of curvature for PA-SA coated magnesium indicates that this sample possesses the highest degree

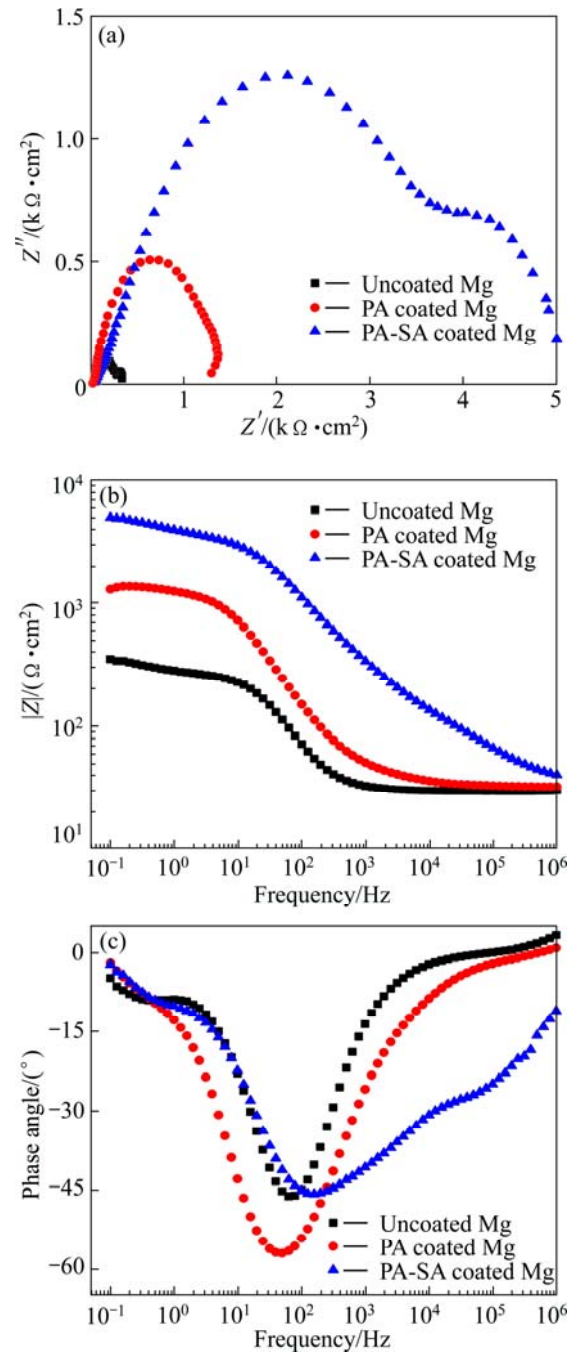


Fig. 7 Nyquist plot (a), $|Z|$ vs frequency (b), and phase angle vs frequency (c) plots (Bode plots) for uncoated and coated magnesium samples

of corrosion protection among all the three types of samples studied in this work. The maximum corrosion protective nature of the PA-SA coated magnesium was confirmed also by noting the highest value of the total impedance ($|Z|$) for PA-SA coated magnesium in the Bode plot (Fig. 7(b)). The high impedance of the coatings prevents the diffusion/penetration of the electrons and ions from the PBS solution to the magnesium substrate and thus reduces the corrosion rate of magnesium. Phase angle is another very important

parameter to evaluate the coating performance. Figure 7(c) shows the variation of phase angle with frequency for the uncoated and coated magnesium samples. As seen in Fig. 7(c), a greater flattening of the maximum for the PA-SA coated magnesium was observed, indicating a greater compactness of the PA-SA coating on magnesium substrate [33].

The analysis of the EIS data provides a deep understanding of electrochemical elements related to the corrosion process, like coating capacitance, coating resistance, double layer capacitance, and charge transfer resistance [34]. These elements are very useful in the analysis of the performance of corrosion protective coatings. For the quantitative estimation of the electrochemical elements, an equivalent circuit model was built based on EIS data measured and their behavior observed. It is imperative that the elements (e.g. resistance, capacitance) selected to develop the equivalent circuit model have a clear physical meaning and are relevant to the corrosion process (Fig. 8). The validity of the equivalent circuit model was established by finding a close correlation between the data generated with the model and data measured experimentally [35]. The theoretical data were generated using Gamry Echem Analyst software. The EIS data of the coated magnesium were best fitted using the equivalent circuit shown in Fig. 8. In this equivalent circuit, R_1 , R_2 , Q_1 , R_3 , Q_2 , R_4 , and C_1 are solution resistance, solution coating interface resistance, solution coating interface constant phase element, coating resistance, coating constant phase element, charge transfer resistance, and double layer capacitance, respectively. For the uncoated magnesium, the best fitted equivalent circuit was observed to be $R_1[R_3\{Q_2(R_4C_1)\}]$. The presence of coating terms (R_3 and Q_2) could be explained by the fact that a very thin layer of magnesium oxide/hydroxide could form on the surface of magnesium [36]. The measured and equivalent circuit fitted impedance spectra for the PA-SA coated magnesium are shown in Fig. 9 as a representative plot. As seen from Fig. 9, there is a good correlation between the measured and the fitted data, which validates the equivalent circuit modeling. The various electrical parameters based on the equivalent circuit modeling for uncoated and coated magnesium samples are given in Table 1. In equivalent circuit modeling, a constant phase element (CPE) was used for the data fitting. CPE is a

‘power law-dependent’ interfacial capacity, which accounts for the topography of imperfections and roughness of the substrate and coating. The impedance of CPE is given as follows [37]:

$$Z_{CPE} = \frac{1}{Y_0(j\omega)^n} \quad (4)$$

where Y_0 is admittance and $n=1$ for ideal capacitor. The CPE can be converted into capacitance by the following expression.

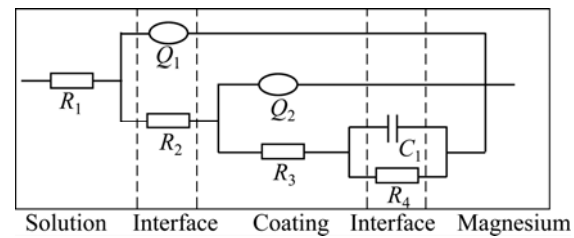


Fig. 8 Equivalent circuit proposed to simulate EIS data for coated magnesium

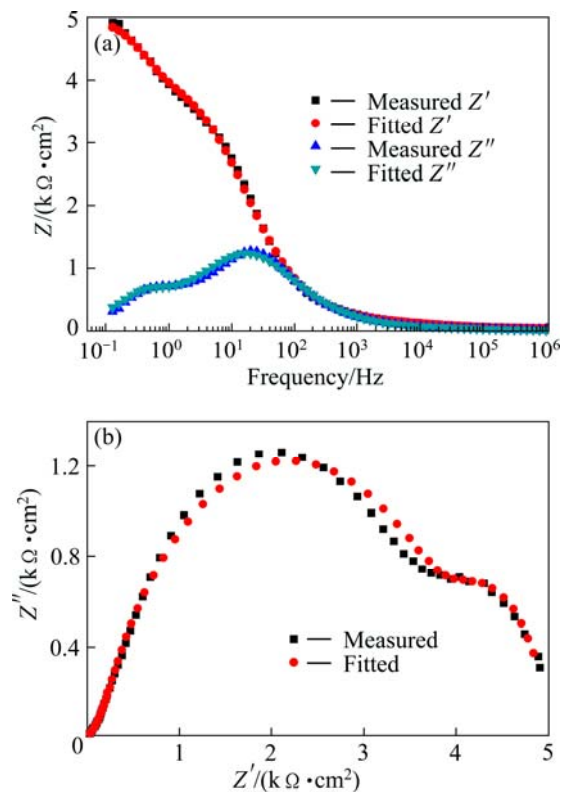


Fig. 9 Measured and fitted Z vs frequency (a) and Z'' vs Z' (b) plots for PA-SA coated magnesium sample

Table 1 Fitting parameters for EIS data obtained for uncoated and coated magnesium samples

Sample	$R_1/$ ($\Omega \cdot \text{cm}^2$)	$R_2/$ ($\Omega \cdot \text{cm}^2$)	$Q_1/$ ($\text{S} \cdot \text{s}^n \cdot \text{n}^{-1}$)	$R_3/$ ($\Omega \cdot \text{cm}^2$)	$Q_2/$ ($\text{S} \cdot \text{s}^n \cdot \text{n}^{-1}$)	$R_4/$ ($\Omega \cdot \text{cm}^2$)	C_1/F
Uncoated Mg	29.9	—	—	2.48×10^2	$1.08 \times 10^{-5}/0.88$	81.2	1.14×10^{-3}
PA coated Mg	32.7	32.1	$2.76 \times 10^{-6}/0.84$	1.26×10^3	$3.45 \times 10^{-6}/0.84$	119	7.24×10^{-4}
PA-SA coated Mg	34.5	181	$8.25 \times 10^{-7}/0.88$	4.05×10^3	$1.13 \times 10^{-6}/0.70$	754	9.54×10^{-5}

$$C = Q(\omega_{\max})^{n-1} \quad (5)$$

where ω_{\max} is the frequency at which the imaginary impedance reaches a maximum for the respective time constant; Q and n are the components of CPE [38]. As evident from Table 1, the total resistance ($R=R_2+R_3+R_4$) of the PA-SA coated magnesium sample is the highest among all the samples, indicating the maximum corrosion protective nature for magnesium substrate.

4 Conclusions

An environment friendly phytic acid conversion coating was formed on the magnesium. The properties of phytic acid coated magnesium were further improved by stearic acid post treatment. The micro-cracks in the phytic acid coated magnesium were filled by soaking in the stearic acid solution that prevents the penetration of reactive ions from solution to magnesium and thus reduces the corrosion of magnesium. The potentiodynamic polarization and electrochemical impedance spectroscopy suggest that stearic acid treated coating provides effective corrosion protection to the magnesium substrate.

Acknowledgement

This research was financially supported by the National Science Foundation through ERC-RMB at NCAT. The authors wish to thank Dr. Y. YUN for his useful discussion and providing access to their research facilities.

References

- [1] EMLEY E F. Principles of magnesium technology [M]. Pergamon Press, 1966.
- [2] WITTE F. The history of biodegradable magnesium implants: A review [J]. *Acta Biomaterialia*, 2010, 6: 1680–1692.
- [3] LORENZ C, BRUNNER J G, KOLLMANNBERGER P, JAAFAR L, FABRY B, VIRTANEN S. Effect of surface pre-treatments on biocompatibility of magnesium [J]. *Acta Biomaterialia*, 2009, 5: 2783–2789.
- [4] ZHANG Y, YAN C, WANG F, LOU H, CAO C. Study on the environmentally friendly anodizing of AZ91D magnesium alloy [J]. *Surface & Coatings Technology*, 2002, 161: 36–43.
- [5] SALUNKE P, SHANOV V, WITTE F. High purity biodegradable magnesium coating for implant application [J]. *Materials Science and Engineering B*, 2011, 176: 1711–1717.
- [6] CHANG J, GUO X, HE S, FU P, PENG L, DING W. Investigation of the corrosion for Mg-xGd-3Y-0.4Zr (x=6, 8, 10, 12wt%) alloys in a peak-aged condition [J]. *Corrosion Science*, 2008, 50: 166–177.
- [7] XIN Y, HU T, CHU P K. In vitro studies of biomedical magnesium alloys in a simulated physiological environment: A review [J]. *Acta Biomaterialia*, 2011, 7: 1452–1459.
- [8] ISHIZAKI T, KUDO R, OMI T, TESHIMA K, SONODA T, SHIGEMATSU I, SAKAMOTO M. Magnesium hydroxide/magnesium phosphate compounds composite coating for corrosion protection of magnesium alloy by a combination process of chemical conversion and steam curing [J]. *Materials Letters*, 2012, 68: 122–125.
- [9] YAO Z, XU Y, LIU Y, WANG D, JIANG Z, WANG F. Structure and corrosion resistance of ZrO₂ ceramic coatings on AZ91D Mg alloys by plasma electrolytic oxidation [J]. *Journal of Alloys and Compounds*, 2011, 509: 8469–8474.
- [10] LI Jian-zhong, HUANG Jiu-gui, TIAN Yan-wen, LIU Chang-sheng. Corrosion action and passivation mechanism of magnesium alloy in fluoride solution [J]. *Transactions of Nonferrous Metals Society of China*, 2009, 19: 50–54.
- [11] SONG Y, SHAN D, CHEN R, ZHANG F, HAN E H. A novel phosphate conversion film on Mg–8.8Li alloy [J]. *Surface & Coatings Technology*, 2009, 203: 1107–1113.
- [12] GRAY J E, LUAN B. Protective coatings on magnesium and its alloys—A critical review [J]. *Journal of Alloys and Compounds*, 2002, 336: 88–113.
- [13] WANG L, CHEN L, YAN Z, WANG H, PENG J. Effect of potassium fluoride on structure and corrosion resistance of plasma electrolytic oxidation films formed on AZ31 magnesium alloy [J]. *Journal of Alloys and Compounds*, 2009, 480: 469–474.
- [14] WANG Q, TAN L, XU W, ZHANG B, YANG K. Dynamic behaviors of a Ca–P coated AZ31B magnesium alloy during in vitro and in vivo degradations [J]. *Materials Science and Engineering B*, 2011, 176: 1718–1726.
- [15] CHONG K Z, SHIH T S. Conversion-coating treatment for magnesium alloys by a permanganate–phosphate solution [J]. *Materials Chemistry and Physics*, 2003, 80: 191–200.
- [16] YFANTISA A, PALOUMPAA I, SCHMEIBERA D, YFANTIS D. Novel corrosion-resistant films for Mg alloys [J]. *Surface & Coatings Technology*, 2002, 151–152: 400–404.
- [17] CUI X, LI Q, LI Y, WANG F, JIN G, DING M. Microstructure and corrosion resistance of phytic acid conversion coatings for magnesium alloy [J]. *Applied Surface Science*, 2008, 255: 2098–2103.
- [18] PAN F, YANG X, ZHANG D. Chemical nature of phytic acid conversion coating on AZ61 magnesium alloy [J]. *Applied Surface Science*, 2009, 255: 8363–8371.
- [19] MAGA J A. Phytate: Its chemistry, occurrence, food interactions, nutritional significance, and methods of analysis [J]. *Journal of Agricultural and Food Chemistry*, 1982, 30: 1–9.
- [20] YE C H, ZHENG Y F, WANG S Q, XI T F, LI Y D. In vitro corrosion and biocompatibility study of phytic acid modified WE43 magnesium alloy [J]. *Applied Surface Science*, 2012, 258: 3420–3427.
- [21] CHERYAN M, RACKIS J J. Phytic acid interactions in food systems [J]. *CRC Critical Reviews in Food Science and Nutrition*, 1980, 13: 297–335.
- [22] LIU Jian-rui, GUO Yi-na, HUANG Wei-dong. Study on the corrosion resistance of phytic acid conversion coating for magnesium alloys [J]. *Surface & Coatings Technology*, 2006, 201: 1536–1541.
- [23] GAO L, ZHANG C, ZHANG M, HUANG X, JIANG X. Phytic acid conversion coating on Mg–Li alloy [J]. *Journal of Alloys and Compounds*, 2009, 485: 789–793.
- [24] CUI X, LI Y, LI Q, JIN G, DING M, WANG F. Influence of phytic acid concentration on performance of phytic acid conversion coatings on the AZ91D magnesium alloy [J]. *Materials Chemistry and Physics*, 2008, 111: 503–507.
- [25] LI Y, WENG W. Surface modification of hydroxyapatite by stearic acid: Characterization and in vitro behaviors [J]. *Journal of Materials Science: Materials in Medicine*, 2008, 19: 19–25.
- [26] NG W F, WONG M H, CHENG F T. Stearic acid coating on magnesium for enhancing corrosion resistance in Hanks' solution [J]. *Surface & Coatings Technology*, 2010, 204: 1823–1830.
- [27] ASTM D3359-02. Standard test methods for measuring adhesion by

- tape test [M]. Philadelphia, PA, USA: ASTM Standards, 2002.
- [28] SCHILLE C, BRAUN M, WENDEL H P, SCHEIDELER L, HORT N, REICHEL H P, SCHWEIZER E, GEIS-GERSTORFER J. Corrosion of experimental magnesium alloys in blood and PBS: A gravimetric and microscopic evaluation [J]. *Materials Science and Engineering B*, 2011, 176: 1797–1801.
- [29] SCHMUTZ P, QUACH-VU N C, GERBER I. Metallic medical implants: Electrochemical characterization of corrosion processes [J]. *The Electrochemical Society Interface*, 2008, 17(2): 35–40.
- [30] STERN M. Electrochemical polarization II. Ferrous-ferric electrode kinetics on stainless steel [J]. *Journal of the Electrochemical Society*, 1957, 104: 559–563.
- [31] FONTANA M G. Corrosion engineering [M]. Tata McGraw-Hill, 2005.
- [32] PEREZ N. Electrochemistry and corrosion science [M]. Springer, USA, 2004.
- [33] BETHENCOURT M, BOTANA F J, CANO M J, MARCOS M, SÁNCHEZ-AMAYA J M, GONZÁLEZ-ROVIRA L. Using EIS to analyse samples of Al–Mg alloy AA5083 treated by thermal activation in cerium salt baths [J]. *Corrosion Science*, 2008, 50: 1376–1384.
- [34] MAHDAVIAN M, ATTAR M M. Another approach in analysis of paint coatings with EIS measurement: Phase angle at high frequencies [J]. *Corrosion Science*, 2006, 48: 4152–4157.
- [35] BONORA P L, DEFLORIAN F, FEDRIZZI L. Electrochemical impedance spectroscopy as a tool for investigating underpaint corrosion [J]. *Electrochimica Acta*, 1996, 41: 1073–1082.
- [36] BRUNELLI K, DABALÀ M, CALLIARI I, MAGRINI M. Effect of HCl pre-treatment on corrosion resistance of cerium-based conversion coatings on magnesium and magnesium alloys [J]. *Corrosion Science*, 2005, 47: 989–1000.
- [37] ALMANZA-WORKMAN A M, RAGHAVAN S, PETROVIC S, GOGOI B, DEYMIER P, MONK D J, ROOP R. Characterization of highly hydrophobic coatings deposited onto preoxidized silicon from water dispersible organosilanes [J]. *Thin Solid Films*, 2003, 423: 77–87.
- [38] LAMAKA S V, MONTEMOR M F, GALIO A F, ZHELUDKEVICH M L, TRINDADE C, DICK L F, FERREIRA M G S. Novel hybrid sol–gel coatings for corrosion protection of AZ31B magnesium alloy [J]. *Electrochimica Acta*, 2008, 53: 4773–4783.

硬脂酸处理提高植酸包覆镁的耐腐蚀性能

R. K. GUPTA, K. MENSAH-DARKWA, J. SANKAR, D. KUMAR

Engineering Research Center for Revolutionizing Metallic Biomaterials (ERC-RMB),
North Carolina A&T State University, 1601 East Market Street, Greensboro, NC-27411, USA

摘要: 将镁浸泡在植酸溶液中, 在其表面形成一层化学转化膜。然后再将其浸泡在硬脂酸溶液中以改善植酸转化膜的显微组织和抗腐蚀性能。经过硬脂酸溶液浸泡处理后, 转化膜未出现裂纹, 试样表面变得光滑。采用电化学方法研究其腐蚀行为。结果表明, 经硬脂酸溶液浸泡处理的试样比未经浸泡处理的和没有转化膜的试样具有更高的耐腐蚀性能。因此, 硬脂酸溶液处理能够增强镁的耐腐蚀性能。

关键词: 镁; 植酸; 硬脂酸; 腐蚀; 阻抗谱

(Edited by Hua YANG)